Nuclear Excitation by Two-Photon Electron Transition

A. V. Volotka,[1,2] A. Surzhykov,[3,4] S. Trotsenko,[1,5] G. Plunien,[6] Th. Stöhlker,[1,5,7] and S. Fritzsche[1,8]
[1]Helmholtz-Institut Jena, D-07743 Jena, Germany
[2]Department of Physics, St. Petersburg State University, 198504 St. Petersburg, Russia
[3]Physikalisch-Technische Bundesanstalt, D-38116 Braunschweig, Germany
[4]Technische Universität Braunschweig, D-38106 Braunschweig, Germany
[5]Institut für Optik und Quantenelektronik, Friedrich-Schiller-Universität, D-07743 Jena, Germany
[6]Institut für Theoretische Physik, Technische Universität Dresden, D-01062 Dresden, Germany
[7]GSI Helmholtzzentrum für Schwerionenforschung, D-64291 Darmstadt, Germany
[8]Theoretisch-Physikalisches Institut, Friedrich-Schiller-Universität, D-07743 Jena, Germany
(Received 20 June 2016; revised manuscript received 25 September 2016; published 5 December 2016)

A new mechanism of nuclear excitation via two-photon electron transitions (NETP) is proposed and studied theoretically. As a generic example, detailed calculations are performed for the $E1E1$ $1s2s\,^1S_0 \to 1s^2\,^1S_0$ two-photon decay of a He-like $^{225}Ac^{87+}$ ion with a resonant excitation of the $3/2+$ nuclear state with an energy of 40.09(5) keV. The probability for such a two-photon decay via the nuclear excitation is found to be $P_{\mathrm{NETP}} = 3.5 \times 10^{-9}$ and, thus, is comparable with other mechanisms, such as nuclear excitation by electron transition and by electron capture. The possibility for the experimental observation of the proposed mechanism is thoroughly discussed.

DOI: 10.1103/PhysRevLett.117.243001

Atomic physics has kept a tenable position for many decades on the foundation and development of our knowledge of nuclear properties. In particular, much information about nuclear spins, nuclear magnetic moments, and mean-square charge radii originate from atomic spectroscopy [1]. Apart from the properties of the nuclear ground or isomeric states, atomic spectroscopy also provides access to the internal nuclear dynamics. For instance, nuclear polarization effects, that arise due to real or virtual nuclear electromagnetic excitations, play a paramount role in an accurate description of muonic atoms [2]. Many years have passed since they were consistently incorporated within the framework of relativistic bound-state QED [3]. Today, the precision in determining the transition energies in highly charged ions requires accounting for the nuclear polarization corrections [4]. In addition, the single nuclear resonances can also be accessed with certain electron transitions.

The accurate determination of nuclear excitation energies and transition rates provides information not only about the nuclear structure of individual isotopes, but also gives access to a number of gripping applications. In the past, for example, two mechanisms were proposed for nuclear excitations by using the techniques of atomic spectroscopy. One, suggested by Morita [5], is known as nuclear excitation by electron transition (NEET). In this process, bound-electron transitions may resonantly induce nearly degenerate nuclear excitations. Another mechanism, the nuclear excitation by electron capture (NEEC), was later suggested by Goldanskii and Namiot [6] and describes the resonant capture of a free electron with the simultaneous excitation of the nucleus. In this latter case, the energy due to the capture of the electron is transferred to a nuclear internal degree of freedom and is subsequently released by the nuclear deexcitation. The scenario of the NEEC process with subsequent x-ray emission relevant for highly charged ions was proposed in Ref. [7]. However, since the nuclear resonances are very narrow, for both mechanisms, NEET and NEEC, it is extremely important to finely adjust the atomic and nuclear transition energies to each other, and this makes the observations of these processes rather challenging. Indeed, only the NEET process has, so far, been verified experimentally for ^{197}Au [8,9], ^{189}Os [10], and ^{193}Ir [11] atoms.

Further studies of the nuclear excitation mechanisms by atomic transition enable us not only to better understand the interactions between the nucleus and electrons and to determine nuclear parameters, but also to open perspectives to a variety of fascinating applications. Among them is the access to low-lying isomeric nuclear excitations, e.g., the isomeric states ^{229m}Th [12–14] and ^{235m}U [15] with an excitation energy of several (tens) eV. Other potential applications can be seen in the isotope separation [5], energy storage [16], and its controlled release [17,18].

In this Letter, we present and discuss a new mechanism for nuclear excitation to which we refer as nuclear excitation by two-photon electron transition (NETP). An electron transition can proceed via emission of not only one photon, but also via simultaneous emission of two photons which share the transition energy. In contrast

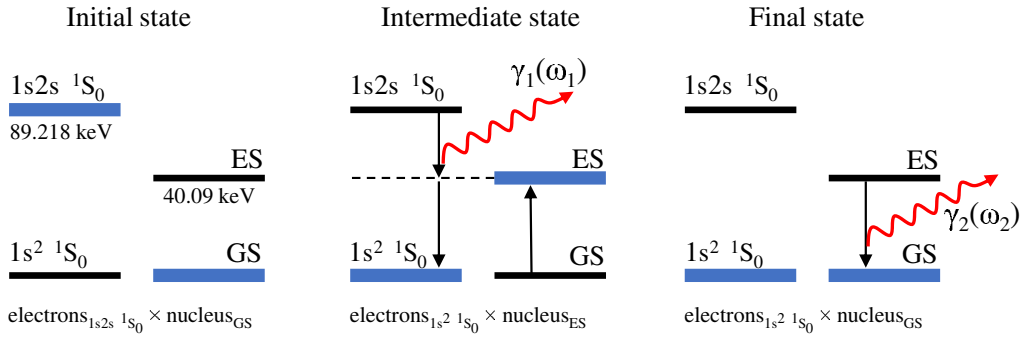

FIG. 1. The mechanism of the nuclear excitation by two-photon electron transition as here explained for a He-like $^{225}Ac^{87+}$ ion. The initial state (left panel), which is characterized by the $1s2s^1S_0$ electronic state and nuclear GS, decays into the final state (right panel), where both the electrons and nucleus are in their ground states $1s^{21}S_0$ and GS, respectively, via the intermediate cascade state (middle panel) with the nucleus being in the ES. The emitted photons γ_1 (electron decay photon) and γ_2 (nuclear fluorescence photon) are depicted by wavy lines with arrows.

to the one-photon transitions, where the photon frequency equals the transition energy, the energy distribution of the spontaneously emitted photons then forms a continuous spectrum. This implies that some of the photons exactly match in their frequency with the nuclear transition energy as long as the nuclear excitation energy is smaller than the total electron transition energy. In this way, a nucleus resonantly absorbs this photon and gets excited. This mechanism can also be understood as the two-photon electron transition in the presence of intermediate (nuclear) cascade states. In the case of NETP, the electrons and the nucleus must be treated as a combined system in which the intermediate cascade state is given by the excited nucleus and the electrons in their ground level. Similarly, as for a pure electronic two-photon decay, the presence of a cascade essentially increases the photon emission intensity in the region of the resonant energy. A key advantage of the NETP process is that, in contrast to the NEET and NEEC, such resonant nuclear excitations may happen for all nuclear levels with an access energy smaller than the total transition energy. In the following, we derive the formulas describing the NETP mechanism and perform calculations especially for the two-photon decay $1s2s^1S_0 \to 1s^{21}S_0$ in a He-like $^{225}Ac^{87+}$ ion. We find that the probability of the two-photon decay via nuclear excitation is surprisingly large $P_{\mathrm{NETP}} = 3.5 \times 10^{-9}$ and comparable with the corresponding NEET probability values P_{NEET} of previously observed [8–11], as well as theoretically proposed, scenarios [19,20].

The NETP process is shown as a two-step process in Fig. 1 in a more picturesque way. For the sake of clarity and without losing generality, we shall refer below always to the He-like $^{225}Ac^{87+}$ ion. In the initial state, the electrons are in the excited state $1s2s^1S_0$ and the nucleus is in its ground state (GS). Then, the electrons undergo the two-photon decay into the ground state $1s^{21}S_0$ via the intermediate state, and the electron decay photon γ_1 with the energy ω_1 is emitted. In the second step, the nucleus, being in the excited state (ES), radiatively decays into its GS with an emission of the nuclear fluorescence photon γ_2 with the energy ω_2. Because of energy conservation, the sum of the photon energies is equal to the total energy ΔE of the electron transition $1s2s^1S_0 \to 1s^{21}S_0$, i.e., $\Delta E = \omega_1 + \omega_2$. The $E1E1$ two-photon transition $1s2s^1S_0 \to 1s^{21}S_0$ in the $^{225}Ac^{87+}$ ion is chosen, here, for various reasons. For such ions, first, the two-photon transition happens rather fast with the total rate $W_{1s2s^1S_0} = 6.002 \times 10^{12}\ \mathrm{s}^{-1}$ [21] and defines the lifetime $\tau_{1s2s^1S_0} = 0.167$ ps of the $1s2s^1S_0$ level completely. Second, the $1s2s^1S_0$ state can be produced quite selectively in collisions of Li-like ions with gas atoms [22,23], and moreover, the two-photon decay energy spectrum has been accurately measured for He-like Sn^{48+} [24] and U^{90+} [25] ions. For the $^{225}Ac^{87+}$ ion, the emitted photons span the frequency region up to the total transition energy $\Delta E = 89.218(2)$ keV [26]. As for the probing nuclear excitation resonance, which lies inside the spanned energy region, we take the $3/2+$ level of the ^{225}Ac nucleus with the excitation energy $\omega_{\mathrm{ES}} = 40.09(5)$ keV [27]. This ES in the case of the neutral actinium atom has a half-lifetime of 0.72(3) ns and decays primarily into the GS via the electric-dipole photon or conversion electron emission with a total conversion coefficient of $\simeq 1$ [28]. For the He-like $^{225}Ac^{87+}$ ion, we, therefore, need to consider only the radiative $E1$ deexcitation channel with the transition rate $W_{\mathrm{ES}} = 0.41 \times 10^9\ \mathrm{s}^{-1}$ and the corresponding linewidth $\Gamma_{\mathrm{ES}} = 2.7 \times 10^{-7}$ eV.

Now, let us provide the theoretical formalism describing the NETP mechanism. While the second-step process is fully determined by the nuclear decay rate itself W_{ES}, the description of the first step, i.e., the nuclear excitation, has to be formulated. Figure 2 displays the Feynman diagrams that describe the first-step process. The corresponding S-matrix element is of third order and can be written (in relativistic units $\hbar = 1$, $c = 1$, $m = 1$) by following the basic principles of QED [29]

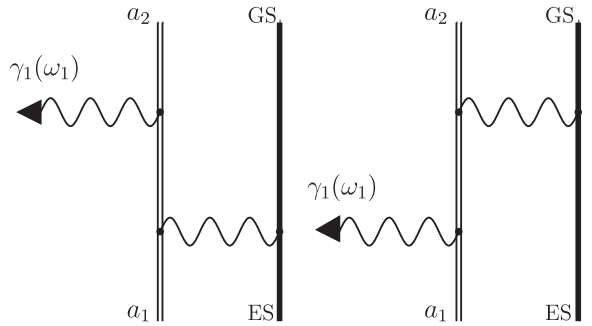

FIG. 2. Feynman diagrams that represent the nuclear excitation during the two-photon electron transition from an initial state a_2 to a final state a_1. The double lines indicate the electron wave functions and electron propagator in the Coulomb field of the nucleus, the heavy lines denote the nucleus in its ground and excited states, and the internal wavy line stays for the photon propagator. The emission of the electron decay photon γ_1 is depicted by the wavy line with the outgoing arrow.

$$
\begin{aligned}
S^{(3)}_{\mathrm{NETP}} = & \frac{1}{\Delta E - \omega_{\mathrm{ES}} - \omega_1 - i(\Gamma_{1s2s^1S_0} + \Gamma_{\mathrm{ES}})/2} \\
& \times \frac{e^2}{4\pi} \int d^3r_1 d^3r_2 d^3R \overline{\psi}_{a_1}(\mathbf{r}_1) \\
& \times \left(\gamma_0 \frac{1}{|\mathbf{r}_1 - \mathbf{R}|} S(\varepsilon_{a_2} - \omega_1, \mathbf{r}_1, \mathbf{r}_2) \gamma^\mu A^*_\mu(\omega_1, \mathbf{r}_2) \right. \\
& \left. + \gamma^\mu A^*_\mu(\omega_1, \mathbf{r}_1) S(\varepsilon_{a_1} + \omega_1, \mathbf{r}_1, \mathbf{r}_2) \gamma_0 \frac{1}{|\mathbf{r}_2 - \mathbf{R}|} \right) \\
& \times \psi_{a_2}(\mathbf{r}_2) \Psi^\dagger_{\mathrm{ES}}(\mathbf{R}) \hat{\rho}_{\mathrm{fluc}}(\mathbf{R}) \Psi_{\mathrm{GS}}(\mathbf{R}), \qquad (1)
\end{aligned}
$$

where $\mathbf{r}_1$ and $\mathbf{r}_2$ are electron coordinates, and $\mathbf{R}$ is the nuclear coordinate. Moreover, $\Gamma_{1s2s^1S_0}$ and Γ_{ES} denote the widths of the $1s2s^1S_0$ electronic level and the nuclear excited state, while the electron wave functions ψ_{a_1} and ψ_{a_2} are bound-state solutions of the Dirac equation for the $1s$ and $2s$ states, respectively. The wave functions Ψ_{GS} and Ψ_{ES} describe the nucleus in its ground and excited states. γ^μ are the Dirac matrices, $S(\omega, \mathbf{r}_1, \mathbf{r}_2)$ is the electron propagator, and $A^*_\mu(\omega, \mathbf{r})$ is the emitted photon wave function. The electron-nucleus interaction acts via the photon propagator which is taken in Coulomb gauge and just restricted to the Coulomb term only. The nuclear charge-density operator $\hat{\rho}_{\mathrm{fluc}}$ characterizes the intrinsic nuclear dynamics due to external electromagnetic excitations and could be decomposed in terms of nuclear multipoles as discussed in Refs. [3,30]. Equation (1) was obtained in the resonant approximation, i.e., $\omega_1 \approx \Delta E - \omega_{\mathrm{ES}}$ and after integration over the time variables in all three vertexes. It should be mentioned that, here, we neglect the interference term between NETP and pure two-photon electron transition, since it turns out to be negligibly small in the present scenario. Finally, we also note that the expression obtained for the S-matrix element is quite general and applies similarly for any other NETP scenario.

To evaluate the S-matrix element in Eq. (1), we follow the standard procedures. Making use of the multipole expansion of the (Coulomb-) photon propagator, we can factorize the nuclear variables and arrive immediately at the matrix element of the nuclear electric transition operator $\hat{Q}_{LM}$

$$
\begin{aligned}
\langle I_{\mathrm{ES}} M_{\mathrm{ES}} | \hat{Q}_{LM} | I_{\mathrm{GS}} M_{\mathrm{GS}} \rangle = & \int d^3R \Psi^\dagger_{\mathrm{ES}}(\mathbf{R}) \hat{\rho}_{\mathrm{fluc}}(\mathbf{R}) \\
& \times \Psi_{\mathrm{GS}}(\mathbf{R}) R^L Y^*_{LM}(\hat{\mathbf{R}}), \qquad (2)
\end{aligned}
$$

where I_{ES}, M_{ES} and I_{GS}, M_{GS} are the nuclear spins and their (magnetic) projections for the excited and ground nuclear states, respectively. Then, the square of the reduced matrix element of the transition operator $\hat{Q}_{LM}$ can be commonly expressed in terms of the reduced transition probability $B(EL; I_{\mathrm{GS}} \to I_{\mathrm{ES}})$. Here, we note that, in accordance with the multipole expansion, the nuclear excitation must have the same type (magnetic or electric) and multipolarity as the one-electron transition, which it replaces in the normal two-photon transition amplitude. If, however, the nuclear and electronic variables are disentangled, we can employ experimental data for the reduced transition probability [27]. The remaining electronic part in the S-matrix element is evaluated here similar to in Ref. [4]. The dual-kinetic-balance finite basis set method [31] is employed to represent the Dirac spectrum in the Coulomb potential of an extended nucleus. Knowing the S-matrix element, one can easily obtain the total rate of the NETP process W_{NETP} as the square of the modulus of the S-matrix element integrated over the energy of the emitted photon ω_1 and multiplied by the total width of the process $\Gamma_{1s2s^1S_0} + \Gamma_{\mathrm{ES}}$. As a result, we find the rate $W_{\mathrm{NETP}} = 0.21 \times 10^5\ \mathrm{s}^{-1}$ for the He-like $^{225}Ac^{87+}$ ion. Furthermore, in order to compare NETP and two-photon probabilities, we define the dimensionless "NETP probability" $P_{\mathrm{NETP}} = W_{\mathrm{NETP}}/W_{1s2s^1S_0}$, which determines the (relative) probability that the decay of the initial atomic state $1s2s^1S_0$ will proceed via the excitation of the nucleus. For the given example, here, we receive $P_{\mathrm{NETP}} = 3.5 \times 10^{-9}$ and, thus, a relative rate that is comparable to the corresponding values for the NEET process, $P_{\mathrm{NEET}} \propto 10^{-7}, \ldots, 10^{-12}$, for most of the proposed examples [19,20]. When the nucleus was excited by the NETP process (cf. Fig. 1), it decayed to the nuclear GS with the transition rate W_{ES}, the linewidth Γ_{ES}, and under the emission of a nuclear fluorescence photon γ_2 with energy $\omega_2 = \omega_{\mathrm{ES}}$.

Now, let us discuss the possibility of the experimental observation of the NETP mechanism. The presence of an additional decay channel significantly modifies the energy spectrum of the usual two-photon emission in the vicinity of the nuclear resonance energy. In Fig. 3, the energy-differential rate for the decay of the $1s2s^1S_0$ state is displayed as a function of the reduced energy $y = \omega/\Delta E$, where ω is the energy carried by one of the emitted photons. As one can see from the figure, the NETP mechanism leads to the appearance of two peaks: the first one at the energy $\omega \approx \omega_1$ and with the width Γ_{ES}, while the second one at $\omega \approx \omega_2$ has the width $\Gamma_{1s2s^1S_0} + \Gamma_{\mathrm{ES}}$. Because

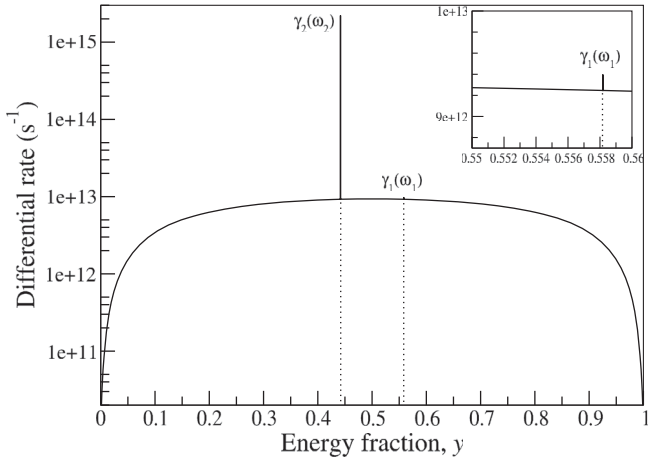

FIG. 3. $1s2s^1S_0 \rightarrow 1s^{21}S_0$ two-photon differential rate plotted as a function of the reduced energy (sharing fraction) y for the He-like $^{225}Ac^{87+}$ ion. The NETP resonances are emphasized by the dotted lines.

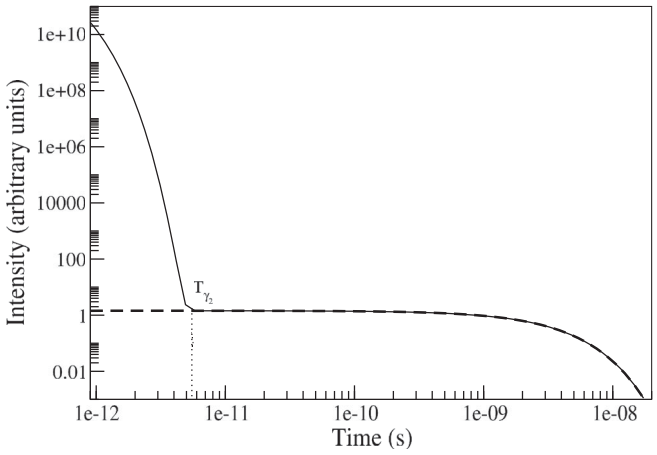

FIG. 4. The overall intensity produced by the decay of the $1s2s^1S_0$ level (solid line) is compared with the intensity of nuclear fluorescence γ_2 photons (dashed line), which are plotted as functions of time in arbitrary units.

of these features of the expected energy sharing of the emitted photons, one can think of two possible options for the experimental observation of the NETP process, which consist of the measurements of either the electron decay γ_1 or nuclear fluorescence γ_2 photons, respectively. If we first consider the observation of photons with frequency ω_1, the emission of the γ_1 photon cannot be separated (in time) from the background signal that is formed by the pure two-photon electronic decay, since both just follow the population of the $1s2s^1S_0$ state. Therefore, the fluorescence intensity of γ_1 photons $I_{\gamma_1}(t)$ decays within the same time, $I_{\gamma_1}(t) \sim \exp(-tW_{1s2s^1S_0})$ and, hence, the main difficulty is to resolve the NETP photons from the background. The signal-to-background ratio can be determined by the partial NETP probability $p_{\mathrm{NETP}}(\Delta)$, which is defined as

$$p_{\mathrm{NETP}}(\Delta) = \frac{W_{\mathrm{NETP}}}{\int_{\omega_1-\Delta/2}^{\omega_1+\Delta/2} dW_{1s2s^1S_0}(\omega)}, \qquad (3)$$

and which describes the probability that a photon with an energy in the range between $\omega_1 - \Delta/2$ and $\omega_1 + \Delta/2$ is emitted via the NETP process. Here, $dW_{1s2s^1S_0}(\omega)$ is the energy-differential rate of the electron two-photon transition, and Δ corresponds to the energy interval that can be distinguished experimentally. For typical x-ray detectors with resolutions of, say, $\Delta = 1$ eV, 10 eV, or 100 eV, we, therefore, get $p_{\mathrm{NETP}}(1\ \mathrm{eV}) = 1 \times 10^{-4}$, $p_{\mathrm{NETP}}(10\ \mathrm{eV}) = 1 \times 10^{-5}$, or $p_{\mathrm{NETP}}(100\ \mathrm{eV}) = 1 \times 10^{-6}$, respectively. Recent progress in developing x-ray detectors enabled one to drastically increase their resolution up to the level of 5 eV or even better, and with a gain in efficiency, cf. Ref. [32]. In this regard, the separation of γ_1 photons might be achieved soon already with present or near-future x-ray technology.

A second set-up of experiments refers to the observation of the nuclear fluorescence γ_2 photons. In contrast to an enhanced emission of γ_1 photons, the γ_2 fluorescence occurs with a certain time delay, which corresponds to the difference between the lifetimes of the $1s2s^1S_0$ state (0.167 ps) and the nuclear excited state (2.4 ns). We can express the intensity of this γ_2 fluorescence as a function of time

$$I_{\gamma_2}(t) \sim \exp(-tW_{\mathrm{ES}}) - \exp(-tW_{1s2s^1S_0}), \qquad (4)$$

and display it in Fig. 4 together with the overall and continuous photon intensity due to the decay of the $1s2s^1S_0$ state (NETP and the pure two-photon decay). As seen from this figure, one can clearly identify the emission of γ_2 photons by observing the fluorescence after some small time delay of, say, $T_{\gamma_2} = 5$ ps, at which the background intensity from the electronic two-photon decay will already be strongly reduced. If we now define the time-dependent NETP probability $p_{\mathrm{NETP}}(T)$ as a relative probability that the photon emitted at time T originates from the NETP process, for times larger than T_{γ_2}, it tends to one, i.e., $p_{\mathrm{NETP}}(T > T_{\gamma_2}) \approx 1$. Thus, the observation of γ_2 photon emissions actually serves us as a signature of the NETP process. In this regard, the measurement of γ_2 photons seems to be presently more feasible for verifying the NETP process.

The latter scenario is planned to be realized at the current GSI (Darmstadt) facility [33]. The initial $1s2s^1S_0$ state can be efficiently produced in the collision of Li-like ions of the given isotope with N_2 gas target via the selective K-shell ionization [23]. Since the $1s2s^1S_0$ state almost exclusively decays via the two-photon transition into the ground state, most of the produced He-like ions contribute to the process under consideration. The x-ray emission will be measured in time coincidences with the detection of the up-charged (He-like) ions, whose efficiency is almost 100%. All these will enable us to measure a very clean spectrum of the two-photon decay [24,25]. In order to observe the delayed nuclear fluorescence photons γ_2, a high-efficiency in-vacuum x-ray detector will be installed to cover a solid angle as large as possible. Fast transitions, that will mostly decay in the vicinity of the gas target, will be shielded in

order to reduce background in the measurement of the delayed photons. In the first experiment, we will compare the measured intensity for the ^{225}Ac and other isotope (e.g., ^{227}Ac) ion beams in order to unambiguously verify the delayed emission of 40 keV photons. Later measurements will record the x-ray intensities at different distances from the gas target, which in turn will allow us to measure the NETP probability P_{NETP} in a way similar to the beam-foil spectroscopy technique [34]. At the experimental storage ring at GSI, beams of $\gtrsim 10^8$ cooled ions can be provided and stored for collisions with the gas-jet target with the areal densities above 10^{14} cm^{-2} [35,36]. Because of the high revolution frequencies of ions in the storage ring (about 2 MHz) and the recurring interaction of ions and target electrons, a very high luminosity can be achieved. Ultimately, we expect stimulating of up to a few hundred NETP fluorescence photons per day of the beam time. This looks very feasible for the successful observation and characterization of the NETP process. Moreover, at the new FAIR accelerator complex, the experiment will profit from the higher luminosity as well as from the ability of the measurements much closer to the ion beam.

In conclusion, here, we present a new mechanism for nuclear excitation by NETP. In contrast to the previously suggested mechanisms, NEET and NEEC, there is no need for observing this mechanism to adjust the electronic and nuclear transition energies to each other. Instead, we can simply utilize the continuous spectrum of the two-photon decay in order to scan for the appropriate nuclear excitation levels. For the given example of the $E1E1$ two-photon transition $1s2s\,^1S_0 \rightarrow 1s^2\,^1S_0$ in the He-like $^{225}Ac^{87+}$ ion, we predict the probability $P_{\mathrm{NETP}} = 3.5 \times 10^{-9}$ when compared with the overall and continuous two-photon emission.

Apart from probing our understanding of the electron-nucleus interaction and nuclear structure, the experimental verification of the NETP process may have far reaching consequences, such as for the search of low-lying isomeric states, for energy storage and its release in a controlled manner [16–18], or elsewhere. We, therefore, hope that this work lays the foundation for developing NETP processes as a sensitive tool at the borderline of atomic and nuclear physics.

This work was supported by Bundesministerium für Bildung und Forschung Project No. 05P15SJFAA.

[1] H.-J. Kluge, Hyperfine Interact. **196**, 295 (2010).
[2] E. Borie and G. A. Rinker, Rev. Mod. Phys. **54**, 67 (1982).
[3] G. Plunien and G. Soff, Phys. Rev. A **51**, 1119 (1995).
[4] A. V. Volotka and G. Plunien, Phys. Rev. Lett. **113**, 023002 (2014).
[5] M. Morita, Prog. Theor. Phys. **49**, 1574 (1973).
[6] V. I. Goldanskii and V. A. Namiot, Phys. Lett. B **62**, 393 (1976).
[7] A. Pálffy, Z. Harman, C. Kozhuharov, C. Brandau, C. H. Keitel, W. Scheid, and T. Stöhlker, Phys. Lett. B **661**, 330 (2008).
[8] S. Kishimoto, Y. Yoda, M. Seto, Y. Kobayashi, S. Kitao, R. Haruki, T. Kawauchi, K. Fukutani, and T. Okano, Phys. Rev. Lett. **85**, 1831 (2000).
[9] S. Kishimoto, Y. Yoda, Y. Kobayashi, S. Kitao, R. Haruki, R. Masuda, and M. Seto, Phys. Rev. C **74**, 031301 (2006).
[10] K. Aoki, K. Hosono, K. Tanimoto, M. Terasawa, H. Yamaoka, M. Tosaki, Y. Ito, A. M. Vlaicu, K. Taniguchi, and J. Tsuji, Phys. Rev. C **64**, 044609 (2001).
[11] S. Kishimoto, Y. Yoda, Y. Kobayashi, S. Kitao, R. Haruki, and M. Seto, Nucl. Phys. **A748**, 3 (2005).
[12] T. T. Inamura and H. Haba, Phys. Rev. C **79**, 034313 (2009).
[13] S. Raeder, V. Sonnenschein, T. Gottwald, I. D. Moore, M. Reponen, S. Rothe, N. Trautmann, and K. Wendt, J. Phys. B **44**, 165005 (2011).
[14] L. von der Wense, B. Seiferle, M. Laatiaoui, J. B. Neumayr, H.-J. Maier, H.-F. Wirth, C. Mokry, J. Runke, K. Eberhardt, C. E. Düllmann *et al.*, Nature (London) **533**, 47 (2016).
[15] P. A. Chodash, J. T. Burke, E. B. Norman, S. C. Wilks, R. J. Casperson, S. E. Fisher, K. S. Holliday, J. R. Jeffries, and M. A. Wakeling, Phys. Rev. C **93**, 034610 (2016).
[16] P. Walker and G. Dracoulis, Nature (London) **399**, 35 (1999).
[17] E. V. Tkalya, Phys. Usp. **48**, 525 (2005).
[18] A. Pálffy, J. Evers, and C. H. Keitel, Phys. Rev. Lett. **99**, 172502 (2007).
[19] E. V. Tkalya, Nucl. Phys. **A539**, 209 (1992).
[20] M. R. Harston, Nucl. Phys. **A690**, 447 (2001).
[21] A. V. Volotka, A. Surzhykov, V. M. Shabaev, and G. Plunien, Phys. Rev. A **83**, 062508 (2011).
[22] S. Fritzsche, P. Indelicato, and T. Stöhlker, J. Phys. B **38**, S707 (2005).
[23] J. Rzadkiewicz, T. Stöhlker, D. Banaś, H. F. Beyer, F. Bosch, C. Brandau, C. Z. Dong, S. Fritzsche, A. Gojska, A. Gumberidze *et al.*, Phys. Rev. A **74**, 012511 (2006).
[24] S. Trotsenko, A. Kumar, A. V. Volotka, D. Banaś, H. F. Beyer, H. Bräuning, S. Fritzsche, A. Gumberidze, S. Hagmann, S. Hess *et al.*, Phys. Rev. Lett. **104**, 033001 (2010).
[25] D. Banaś, A. Gumberidze, S. Trotsenko, A. V. Volotka, A. Surzhykov, H. F. Beyer, F. Bosch, A. Bräuning-Demian, S. Fritzsche, S. Hagmann *et al.*, Phys. Rev. A **87**, 062510 (2013).
[26] A. N. Artemyev, V. M. Shabaev, V. A. Yerokhin, G. Plunien, and G. Soff, Phys. Rev. A **71**, 062104 (2005).
[27] A. K. Jain, R. Raut, and J. K. Tuli, Nucl. Data Sheets **110**, 1409 (2009).
[28] T. Ishii, I. Ahmad, J. E. Gindler, A. M. Friedman, R. R. Chasman, and S. B. Kaufman, Nucl. Phys. **A444**, 237 (1985).
[29] V. B. Berestetsky, E. M. Lifshitz, and L. P. Pitaevsky, *Quantum Electrodynamics* (Pergamon Press, Oxford, 1982).
[30] G. Plunien, B. Müller, W. Greiner, and G. Soff, Phys. Rev. A **43**, 5853 (1991).
[31] V. M. Shabaev, I. I. Tupitsyn, V. A. Yerokhin, G. Plunien, and G. Soff, Phys. Rev. Lett. **93**, 130405 (2004).
[32] D. Hengstler, M. Keller, C. Schötz, J. Geist, M. Krantz, S. Kempf, L. Gastaldo, A. Fleischmann, T. Gassner, G. Weber *et al.*, Phys. Scr. **T166**, 014054 (2015).
[33] S. Trotsenko *et al.*, letter of intent for GSI/FAIR (2016).
[34] E. Träbert, Phys. Scr. **78**, 038103 (2008).
[35] N. Petridis, A. Kalinin, and R. E. Grisenti, Internal Jet Target@HESR (FAIR), Report No. 3_02, 2014 (unpublished).
[36] N. Petridis, R. E. Grisenti, Y. A. Litvinov, and T. Stöhlker, Phys. Scr. **T166**, 014051 (2015).